CORRELATION OF THE VISIBLE AND RADAR STRATIGRAPHIC RECORDS OF MARS' NPLD

P. Becerra[1], D. Nunes[2], I. Smith[3], M.M. Sori[4], Y. Brouet[1], N. Thomas[1]; [1]Physikalisches Institut, Universität Bern, Switzerland, [2]Jet Propulsion Laboratory, Pasadena, USA, [3]Planetary Science Institute, Colorado, USA, [4]University of Arizona, Tucson, USA.

Introduction: A long-standing problem in Mars Polar Science is the interpretation of the stratigraphic record preserved in Mars' icy North Polar Layered Deposits (NPLD) [1] (Fig. 1a), whose accumulation patterns of ice and dust have long been thought to associate with recent climatic changes forced by variations of the planet's astronomical parameters [2,3]. The internal layering of the NPLD is visible in exposures within a series of spiraling troughs that dissect the NPLD dome (Fig. 1a,b). Studies have relied on remote images of these troughs to map the stratigraphy [4–8] and search for a connection between NPLD accumulation and astronomical forcing [9–12]. Sub-surface radar sounding has also proved invaluable in observing the internal structure of the deposits. The SHARAD instrument detects changes in dielectric properties with depth. As these vary for beds with different amounts of dust, layering is observed as radar reflections [13].

The optical and radar-based stratigraphies have predominantly been studied in isolation. In terrestrial climate science, orbital climate forcing was ultimately confirmed by the correlation of various datasets [14], suggesting that this integration is necessary to unlock a complete climate record for the NPLD. In general, both radar and optical layers are assumed to result from varying amounts of dust impurities in water ice [15] (assuming negligible and uniform porosity). Christian et al. [16] attempted the first quantitative correlation and found a general agreement between properties of radar reflectors and visible layers, such as bed geometry and wavelength. This result provided evidence that the same physical quantity (potentially dust fraction) controls the formation of both radar reflectors and protruding strata. However, the unique correlation of a particular radar reflector with one visible layer or layer-packet remains an open problem.

Here, we present our approach to this correlation by modeling the SHARAD propagation through layered media whose electrical properties are based on topographic profiles of bed exposures. These are extracted from Digital Terrain Models (DTMs) made with images from the HiRISE instrument. The objective is to test the hypothesis that highly protruding 'marker beds' have sufficient dielectric contrast with the neighboring beds to create radar reflections, thus associating individual reflectors to visible layers. These profiles can inform orbitally-forced accumulation models [17,18], that could unlock the temporal climate record of the NPLD.

Methods: The goal of the data integration is to obtain dust content vs. depth profiles that can be directly compared to the output of accumulation models. Our approach: (1) Extract HiRISE-based profiles of topographic expression at various sites. (2) Model the radar wave propagation through synthetic profiles of the real part of the electric permittivity (ε), constructed based on the HiRISE topography and assumptions about the value of ε for marker beds. (3) Correlate these profiles to real SHARAD data using spectral analysis and pattern-matching algorithms. This correlation would result in HiRISE-SHARAD stratigraphic profiles of ε, which can be transformed to fractional dust-content [19] that can constrain accumulation models.

We first measure 1D profiles of topography down the trough face in the DTMs and calculate how much a bed protrudes from an average linear fit to the surface within a particular window (these protrusion profiles (Fig. 2a) were used by [8] to correlate layer exposures across the NPLD; the complete procedure for their extraction is explained therein). The profiles are then used to generate a depth profile of ε based on an empirical model that relates protrusion to ε by varying the ε of marker beds between that of pure ice (3.00–3.15) and higher values up to 5 (Fig. 2b) – an unusually high dust fraction (~50%) compared to the bulk (5%) of the NPLD [20, 21]. Our hypothesis is that the dust that affects the dielectric response also affects layer strength and protrusion [8,18]. With the radar-propagation model of [15], we then generate synthetic radargrams with subsurface interfaces at the location of the simulated marker beds (Fig. 2c), which we can compare directly to the SHARAD reflection trace at the closest point possible to the location on the trough wall were the protrusion profiles were extracted.

Preliminary Results: The synthetic radar profile of fig. 2c simulates the SHARAD reflection trace through a ε-profile guided by the protrusion profile of site N11 (Fig. 1a), which begins at a depth of ~200 m. We chose this site first because of its favorable geometry with respect to the SHARAD observations. The marker beds here were assigned a ε of 5, while the background a ε of 3.15. Fig. 2c shows that thick protrusion peaks (>12 m) are resolvable between radar reflections, while thinner layers may not be distinguishable because of the radar's intrinsic resolution.

The visual comparison of the synthetic radargram with the corresponding SHARAD observation (Fig. 2d) shows a similar pattern and similar number of reflections to the model between 1.5 and 5.0 μs (~100–400 m in depth) in the real radargram. This comparison supports the hypothesis that synthetic radargrams generated with this method are comparable to actual

observations, although no definitive ties between unique beds have been made at this time.

Our first attempts at correlation with the pattern-matching algorithm known as dynamic-time warping (DTW) [8,22] have promising results. DTW finds the best match between two time-varying functions by 'tuning' one to the other and maximizing the covariance between the two. In this case, the tuned function is the synthetic radargram, and the forcing function is the real one. The statistical significance is then found by repeating the process with random functions and comparing the covariances (see [8] and [22] for details). The cross-correlation coefficient and the Monte Carlo statistical significance parameter are high for the case of site N11 (0.937 and 92% respectively), although the uncertainty also remains high because only one SHARAD radargram, instead of an average of many intersecting ones, is used [23].

Future Work: Our preliminary investigations have promising results. We will extend this study and generate synthetic radar profiles based on different empirical ε–protrusion relations at each site shown in fig. 1a. We will select 2–10 SHARAD observations to average radargrams of depth vs. power profiles (e.g. Fig. 2d) at locations near each trough wall, so that each site has a representative radar and protrusion profile. To continue the correlation efforts, we will use various methods: Wavelet analysis [12,24] will estimate similarities between profiles by comparing their spectral properties. Standard cross-correlation calculations will complement the DTW method in order to quantify the degree of correlation without tuning (given that the synthetic radargrams are the result of propagation through a layered medium at the same location as the observations). Further work involves comparing the integrated stratigraphy with formation models controlled by orbital cycles [e.g. 18].

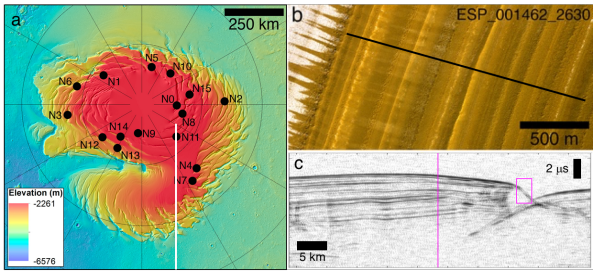

Figure 1. (a) Topographic map of the NPLD. Dots = locations of study sites and HiRISE DTMs from [9]. Line = ground track of SHARAD radargram in (c). (b) HiRISE image of exposed layers in an NPLD trough. (c) SHARAD radargram 492802. Pink square marks the approximate location of N11. The pink line indicates the trace of the profile of Fig. 2d.

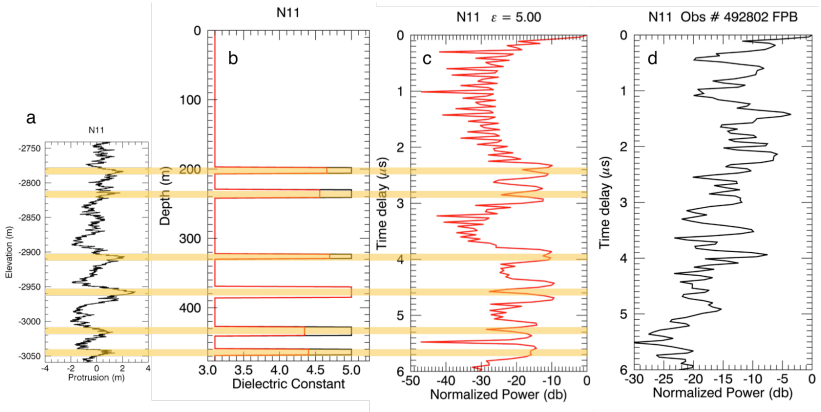

Figure 2. (a) Protrusion profile of the exposure at site N11. Yellow bands indicate 'marker beds'. (b) ε-profile based on (a). (c) Synthetic radar profile produced by wave propagation through marker beds of 2b using a simple compressed pulse. Both top and bottom marker bed interfaces are resolved. (d) SHARAD radar profile near site N11. Delay times and power for both (c) and (d) are referenced to the first arrival of the surface reflection.

References

[1] Clifford et al. Icarus 225 (2013) [2] Cutts, JGR 78 (1973) [3] Cutts et al. Science 194 (1976) [4] Fishbaugh et al. JGR 111 (2006) [5] Tanaka et al. Icarus 196 (2008) [6] Fishbaugh et al. GRL 37 (2010) [7] Limaye et al. JGR 117 (2012) [8] Becerra et al. JGR 121 (2016) [9] Laskar et al. Nature 419 (2002) [10] Milkovich & Head, JGR 110 (2005) [11] Perron & Huybers, Geology 37 (2009) [12] Becerra et al. GRL 44 (2017) [13] Putzig et al. Icarus 204 (2009) [14] Imbrie, Icarus 50 (1982) [15] Nunes & Phillips, JGR 111 (2006) [16] Christian et al. Icarus 226 (2013) [17] Levrard et al. JGR 112 (2007) [18] Hvidberg et al. Icarus 221 (2012) [19] Stillman et al. J.Phys.Chem. 114 (2010) [20] Grima et al. GRL 36 (2009) [21] Lalich & Holt, GRL 44 (2017) [22] Sori et al. Icarus 235 (2014) [23] Nunes et al. LPSC XLIX (2018) [24] Torrence & Compo, Bull. Am. Met. Soc. 79 (1998)